Journal of Chromatography, 644 (1993) 161–174
Elsevier Science Publishers B.V., Amsterdam

CHROM. 25 063

Axial temperature effects in electromigration

Bohuslav Gaš

Faculty of Science, Charles University, Albertov 2030, 128 40 Prague 2 (Czech Republic)

(First received August 10th, 1992; revised manuscript received March 12th, 1993)

ABSTRACT

A model of electrophoretic migration that is influenced by generated Joule heat is presented. The model takes into account the axial flux of the heat. It is shown that the mutual influence of non-equilibrium fluxes of mass and heat may lead to new phenomena: oscillation of the concentration profile on concentration boundaries and changes in concentration of the electrolytes (either an increase or a decrease) appearing at sites of jumps of the radial heat flux of the capillary tube. The theoretical results are supported by experiments.

INTRODUCTION

The production of heat is an inherent phenomenon accompanying all electromigration separation methods. The heat is generated by ohmic resistance of the electrolyte due to flow of the electric current and, in consequence, the temperature of the separation media is increased. The heat is generated in the whole volume of the separation media but it is transported outside by the walls of the column. It causes a non-homogeneous radial distribution of the temperature in the separation column. Electrophoretic mobility, which plays a significant role in electromigration methods, is strongly influenced by the temperature. Therefore, the temperature gradient causes radial variations in the migration velocity profile and, in consequence, a decrease in separation efficiency [1–9].

The loss of heat by the walls of the separation column is dependent on the overall heat transfer through the capillary walls. This heat transfer may vary in various parts of the column owing to different thermal conductivities and the heat transfer coefficient of the walls. Additionally, different electric conductivities of various sites of the solution in the capillary column (*e.g.*, in distinctive isotachophoretic zones or in any disturbances in the axial concentration profile) also cause different Joule heat powers and different temperatures of the sites. Both will cause an axial flux of the heat.

It should be emphasized that the axial variation of the heat transfer through the column walls can be distinguished, especially in junctions of non-thermostated column tubing. In consequence, the axial variation of temperature can reach several tens of degrees and can exceed the radial variation. In all studies [1–9] dealing with the effects of temperature gradients on the efficiency of electrophoretic separations, the axial flux of heat was omitted. This neglect may be acceptable in cases of thermal band broadening of peaks moving relatively quickly by electrophoretic or electroosmotic velocity in a homogenous and concentrated background buffer, but may fail in cases of concentration boundaries. Such a concentration boundary moves in a capillary relatively slowly owing to the concentration dependence of the transference numbers of ions on both sides of the boundary [10,11].

Generally, the transference numbers are also dependent on temperature. It will be shown in this paper that the temperature dependence of transference numbers gives rise to an interesting phenomenon, *i.e.*, moving oscillation of the

0021-9673/93/$06.00

concentration profile of the concentration boundary. Additionally, owing to the temperature dependence of the transference numbers, the axial jumps in the heat transfer coefficient of the capillary walls and consequent axial jumps in the temperature of the buffer will cause an increase or decrease in concentration at sites of the jumps.

The aim of this work was to obtain a theoretical description, computer solution and experimental support of a model of electromigration separation processes taking into account the mutual influence of the mass and heat fluxes. This paper is organized as follows: formulation of a general mathematical model of temperature-influenced electromigration; formulation of a simplified mathematical model of temperature influenced electromigration assuming a homogeneous radial distribution of temperature; numerical solution of both models; formulation of a linearized modification of the simplified model and both its analytical and numerical solution; and experimental verification.

MATHEMATICAL MODELS

General model of temperature-influenced electromigration

Let us consider a capillary tube as a separation column with length L and inner radius R filled by a solution of n strong ions. Let the axial x coordinate be the axis of the capillary and let an outer electric field act in the direction of x coordinate. Further, we do not consider bulk convection or electrosmotic flow in the column.

The system is cylindrically symmetrical, therefore it is possible to cope with only two spatial coordinates, namely x and r, where r is the radial coordinate of the capillary tube. The concentration $c_i = c_i(x, r, t)$ of the ith ion and the temperature $T = T(x, r, t)$ in the column will be functions of the three variables, *i.e.*, the spatial x and r coordinates, $x \in \langle 0, L \rangle$, $r \in \langle 0, R \rangle$, and the time t, $t \geq 0$.

Each ion inside the column is affected by two forces: the chemical potential gradient of the ion and the electric potential gradient. In a very dilute solution, eventual cross-effects between fluxes of different ions can be neglected [12] and a gradient of concentration can be used instead of the chemical potential gradient. The matter flux $\boldsymbol{J}_i(x, r, t)$ of the ith ion in the capillary tube is a vector composed of two components, $J_{i,x}(x, r, t)$ and $J_{i,r}(x, r, t)$. Assuming proportionality between fluxes and forces, the matter fluxes are [12]

$$\boldsymbol{J}_i = -D_i \operatorname{grad} c_i - \operatorname{sgn}(z_i) u_i c_i \operatorname{grad} \phi \,, \quad i = 1, \ldots, n \tag{1}$$

where z_i, D_i and u_i are the relative charge number, diffusion coefficient and ionic mobility of the ith ion, respectively, ϕ is the electric potential and grad is the gradient of a scalar function in cylindrical coordinates.

Fluxes of charged particles are related to the flow of the electric current. It must be realized that the current density $\boldsymbol{j}$ is also a vector, which is dependent on x, r and t coordinates:

$$\boldsymbol{j} = F \sum_{k=1}^{n} z_k \boldsymbol{J}_k \tag{2}$$

where F is the Faraday constant. Eliminating the potential gradient from eqn. 1 using eqn. 2, we have

$$\boldsymbol{J}_i = -D_i \operatorname{grad} c_i + \frac{\operatorname{sgn}(z_i) c_i u_i}{\kappa} \left(\boldsymbol{j} + F \sum_{k=1}^{n} z_k D_k \operatorname{grad} c_k \right) \tag{3}$$

where κ is the specific conductivity:

$$\kappa = F \sum_{k=1}^{n} |z_k| c_k u_k \tag{4}$$

The continuity equation, $\partial c_i / \partial t = -\operatorname{div} \boldsymbol{J}_i$ (where div is the divergence of a vector) expresses the mass balance at each point in the capillary tube. In our system it can be written as

$$\frac{\partial c_i}{\partial t} = \operatorname{div} \left[D_i \operatorname{grad} c_i - \frac{\operatorname{sgn}(z_i) c_i u_i}{\kappa} \left(\boldsymbol{j} + F \sum_{k=1}^{n} z_k D_k \operatorname{grad} c_k \right) \right] \tag{5}$$

The vector heat flux, $\boldsymbol{J}_T(x, r, t)$, in the capillary tube is composed of two components, $J_{T,x}(x, r, t)$ and $J_{T,r}(x, r, t)$, and, neglecting the Soret

effect [13], can be described by a phenomenological Fourier law [14,15]:

$$J_T = -K \operatorname{grad} T \tag{6}$$

where K is the thermal conductivity. The relevance of the neglect of the Soret effect is discussed in the Appendix.

The Joule heat power, w_g, generated by the electric current density, j, in solution per unit volume is $w_g = |j|^2/\kappa$. This term appears as the source term in the following equation which can be written for temperature:

$$\rho_m c_h \frac{\partial T}{\partial t} = \operatorname{div}(K \operatorname{grad} T) + \frac{|j|^2}{\kappa} \tag{7}$$

where ρ_m is the mass density and c_h is the heat capacity of the solution.

It should be further considered that many physico-chemical properties depend on temperature and/or concentration. For the correct description of a real situation, these dependences should be taken into account.

Mobilities, u_i, depend strongly on concentrations and temperature, *i.e.*, $u_i = u_i(c_1, \ldots, c_n, T)$. The limiting ionic mobility, u_i^0, which is the mobility of an ion at infinite dilution, varies owing to changes in the interaction between solvent molecules and the ions, and between the solvent molecules themselves. The main part of this variation is caused by the change in viscosity of the solvent. This can be expressed as the Walden rule [16], which states that the product of the limiting mobility and the viscosity of the solvent is approximately constant. For practical reasons, the temperature dependence of the limiting mobility can be expressed as a polynomial function of the temperature. Constants of the polynomial can easily be obtained by fitting from available experimental data.

The Debye–Hückel–Onsager theory [17] describes the temperature dependence of the electrophoretic and relaxation effects influencing the mobility in a finite concentration. The Onsager limiting law can be written in the form

$$u_i = u_i^0 - (Au_i^0 + B)\sqrt{I_S} \tag{8}$$

where I_S is the ionic strength and A and B are terms corresponding to the relaxation and electrophoretic effects, respectively. They are independent of concentration, but dependent on temperature, permittivity and viscosity of the solvent. The temperature dependence of the terms A and B may also be expressed, in a not very broad temperature interval, as a polynomial function.

The concentration dependence of the diffusion coefficients can be neglected with good precision. For example, the diffusion coefficient of NaCl in aqueous solution at 25°C increases by about 0.5% on changing the concentration from infinite dilution to 10 mol m^{-3} [16]. However, the diffusion coefficients of ions depend strongly on temperature, *i.e.*, $D_i = D_i(T)$. There is no theory describing the temperature dependence of diffusion coefficients in liquids precisely. Nevertheless, for our purposes the simplest hydrodynamic theory can be used. For diffusion of the large, spherically symmetrical ith ion with diameter r_i in a solvent with small molecules, the Stokes–Einstein equation [18] holds for the diffusion coefficient D_i:

$$D_i = \frac{k(T + 273)}{6\pi\eta r_i} \tag{9}$$

where k is the Boltzmann constant, T is the temperature expressed in °C and η is the viscosity coefficient of the solvent. As the temperature dependence of the viscosity of liquids is approximately exponential [18], it can be written in accordance with the Arrhenius relationship for the viscosity coefficient:

$$\eta = A_{visc} \exp\left[\frac{E_{visc}}{k(T + 273)}\right] \tag{10}$$

where A_{visc} and E_{visc} are constants of the solvent independent of temperature. Hence, taking into account eqns. 9 and 10, the temperature dependence of the diffusion coefficient of the ith ion is

$$D_i = K_{i,visc}(T + 273) \exp\left[-\frac{E_{visc}}{k(T + 273)}\right] \tag{11}$$

where $K_{i,visc}$ is a constant of the ith ion. Again, the parameters A_{visc}, E_{visc} and $K_{i,visc}$ can be obtained by fitting from available experimental data.

For a complete description of electromigration including the temperature effects, the equations

describing the temperature and/or concentration dependences of mobilities, diffusion coefficients and thermal conductivities must be added to eqns. 5 and 7. These equations, together with appropriate initial and boundary conditions, form the general model of temperature-influenced electromigration. The initial condition is an initial distribution of concentration and temperature in a column. It is natural to assume a homogeneous initial radial distribution of concentration of all ions in the tube and a constant initial temperature equal to the temperature of the surroundings T_S at time $t = 0$ in the whole column, *i.e.*,

$$c_i(x, r, 0) = C_i(x), \quad T(x, r, 0) = T_S,$$
$$x \in \langle 0, L \rangle, \quad r \in \langle 0, R \rangle \tag{12}$$

where $C_i(x)$ is the initial axial concentration distribution of the ith ion.

The boundary condition at the centre line $r = 0$ reflects a cylindrical symmetry of the problem; therefore,

$$\frac{\partial c_i}{\partial r}(x, 0, t) = 0 \quad \text{and} \quad \frac{\partial T}{\partial r}(x, 0, t) = 0,$$
$$x \in \langle 0, L \rangle, \quad t > 0 \tag{13}$$

At the capillary wall, where $r = R$, heat is transported outside the column. The overall radial heat flux will be proportional to the difference between the temperature of the inner wall and the temperature of the surroundings, hence the boundary condition is

$$-K \cdot \frac{\partial T}{\partial r}(x, R, t) = h_0[T(x, R, t) - T_S],$$
$$x \in \langle 0, L \rangle, \quad t > 0 \tag{14}$$

where h_0 is the overall heat transfer coefficient. If the column is formed of a simple capillary tube with an inner radius R and an outer radius R_0, the overall heat transfer coefficient is [19]

$$h_0 = \frac{1}{R} \cdot \frac{1}{[\ln(R/R_0)/K_W] + 1/R_0 h_S} \tag{15}$$

where K_W is the thermal conductivity of the capillary wall and h_S is the surface heat transfer coefficient. The surface heat transfer coefficient h_S is a function of the cooling properties of the surroundings and the surface temperature of the outer capillary wall. Gobie and Ivory [8] calculated its value for various cooling conditions and found $h_S \approx 130$ or $h_S \approx 3200$ W m^{-2} K^{-1} for an air-cooled or liquid-cooled capillary, respectively. Generally, it will be assumed that $h_S = h_S(x)$ and $h_0 = h_0(x)$.

The boundary conditions for concentrations at the boundary $r = R$ are

$$\frac{\partial c_i}{\partial r}(x, R, t) = 0, \quad x \in \langle 0, L \rangle, \quad t > 0 \tag{16}$$

which means that matter cannot be transported through the walls.

Boundary conditions at the boundaries $x = 0$ and $x = L$ should reflect the fact that here we are interested in phenomena taking place inside a capillary tube. Real boundaries originating at connections of the capillary column to electrode vessels would bring another complexity to modelling. Therefore, it will be convenient to adopt boundary conditions:

$$\frac{\partial c_i}{\partial x}(0, r, t) = 0 \quad \frac{\partial T}{\partial x}(0, r, t) = 0$$
$$\frac{\partial c_i}{\partial x}(L, r, t) = 0 \quad \frac{\partial T}{\partial x}(L, r, t) = 0$$
$$r \in \langle 0, R \rangle, \quad t > 0 \tag{17}$$

Analogous equations for transport of mass to the set of eqns. 5 can be written for electromigration of weak electrolytes. In this case, for the relevant description of temperature-influenced electromigration, the temperature dependence of the dissociation constants should also be known.

Simplified model of temperature influenced electromigration

The solution of the general eqns. 5 and 7, assuming the initial and boundary conditions 12–14, 16 and 17, is very complex, hence it would be beneficial to find a simplification of the model.

Owing to diverse thermal conductivity and the overall heat transfer coefficient of the various parts of the column walls, it can be expected that an axial temperature profile may vary considerably in different parts of the column. Especially in junctions of column tubing or in junc-

tions of liquid-cooled and air-cooled parts of a capillary tube the overall heat flux outside the column exhibits large jumps. The axial jumps in temperature may easily reach several tens of degrees. Other reasons for a non-constant axial temperature distribution are different conductivities or concentrations of solutions in various parts of the capillary.

On the other hand, the radial temperature gradient often hardly reaches a few degrees under working conditions typical in CZE or ITP.

From this point of view, if only axial effects are to be studied, it will be not too far from reality to assume uniform radial distributions of concentration and temperature, *i.e.*, $c_i = c_i(x, t)$ and $T = T(x, t)$. Hence eqns. 5 will have the form

$$\frac{\partial c_i}{\partial t} = \frac{\partial}{\partial x}\left[D_i \cdot \frac{\partial c_i}{\partial x} - \frac{\mathrm{sgn}(z_i) c_i u_i}{\kappa}\left(j + F\sum_{k=1}^{n} z_k D_k \cdot \frac{\partial c_k}{\partial x}\right)\right] \quad (18)$$

The current density j is now not a function of r and consequently not a function of x, hence $j = j(t)$. If the electric current is controlled by an electronic regulator to a constant value I, then $j = I/(\pi R^2)$.

In the simplest case of a uni–univalent electrolyte, $i = 1,2$ and the electroneutrality condition relates $c_1 = c_2$. Denoting $c = c_1 = c_2$, $z_1 = 1$ and $z_2 = -1$, the set of eqns. 18 is reduced to one equation:

$$\frac{\partial c}{\partial t} = \frac{\partial}{\partial x}\left\{D_1 \cdot \frac{\partial c}{\partial x} - \frac{u_1}{u_1 + u_2}\left[\frac{j}{F} + (D_1 - D_2)\frac{\partial c}{\partial x}\right]\right\} \quad (19)$$

which can be rewritten as

$$\frac{\partial c}{\partial t} = \frac{\partial}{\partial x}\left(D \cdot \frac{\partial c}{\partial x} - \frac{u_1}{u_1 + u_2} \cdot \frac{j}{F}\right) \quad (20)$$

denoting $D = (D_1 u_2 + D_2 u_1)/(u_1 + u_2)$.

Eqn. 14 can no longer be a boundary condition but an additional term describing a heat loss. Therefore, the analogy of eqn. 7 will now be (using the simple relationship between the surface and volume of a cylinder)

$$\rho_m c_h \cdot \frac{\partial T}{\partial t} = \frac{\partial}{\partial x}\left(K \cdot \frac{\partial T}{\partial x}\right) + \frac{j^2}{\kappa} - h_0 \cdot \frac{2}{R}(T - T_S) \quad (21)$$

The initial and boundary conditions can be analogous to eqns. 12 and 17:

$$c_i(x, 0) = c_i(x), \quad T(x, 0) = T_S, \quad x \in \langle 0, L \rangle \quad (22)$$

$$\frac{\partial c_i}{\partial x}(0, t) = 0, \quad \frac{\partial T}{\partial x}(0, t) = 0, \quad t > 0 \quad (23)$$

In fact, the isolated set of eqns. 18 gives a complete description of the migration of strong ions in an electric field at constant temperature. This set of equations was solved numerically by Dose and Guiochon [20] for several strong electrolytes.

It is evident that an analytical solution of eqns. 5 and 7 or even eqns. 20 and 21 can hardly be found, and therefore a numerical solution must be coped with.

EXPERIMENTAL

The numerical solution of the partial differential equations was performed by the method of lines. It consisted in discretizing spatial derivatives at a set of grid points to generate a set of ordinary differential equations with time as the independent variable. The finite-difference approximation is based on the first-order symmetrical difference approximation for both first and second derivatives. The Hamming's modification of the fourth-order predictor–corrector method [21] was used for the solution of the resulting set of ordinary differential equations.

The algorithm solving dynamics of electromigration was programmed in Pascal and can run on IBM PC computers. Simulation results can be displayed in graphical form.

The electromigration experiments were done on a one-column isotachophoretic analyser consisting of the hydraulic part from an Agrofor system (JZD, Odra Krmelín, Czech Republic) and a high-frequency contactless detector [22]. The capillaries were made of PTFE. Sodium chloride (Lachema, Brno, Czech Republic) was of analytical-reagent grade and bromophenol blue (Lachema) was of purum grade. No addi-

tives were added to solutions to decrease the electroosmotic flow.

RESULTS AND DISCUSSION

Further considerations will be limited to the temperature-influenced electromigration of binary uni–univalent electrolytes.

Stockmayer [11] derived that the concentration boundary of a binary electrolyte moves in an electric field in a capillary due to concentration dependence of the transference numbers. He showed that if this dependence is linear, the moving concentration boundary is simply shifted by a constant velocity and spread by diffusion. If the dependence is non-linear, additional distortion of the boundary shape takes place.

It will be further shown that if the temperature influence is considered, the moving concentration boundary can have a different character. From comparison with experiments, an available and well defined electrolyte system should be chosen. NaCl was considered as such an electrolyte because Na^+ and Cl^- ions have different mobilities and different temperature dependences of the mobility. Additionally, detailed data on the mobility and diffusion of these ions are readily available. In the following text, the subscripts 1 and 2 represent Na^+ and Cl^-, respectively. Assuming a polynomial temperature dependence of limiting mobilities and using published experimental data [16,23], the following concentration and temperature dependences of the mobilities in aqueous solution were obtained by fitting:

$$A = 0.2209 + 3.325 \cdot 10^{-4}T + 1.640 \cdot 10^{-6}T^2 \quad (24)$$

$$B = 31.45 + 0.6304T + 0.01428T^2 \quad (25)$$

$$L_1 = 25.58 + 0.9000T + 3.852 \cdot 10^{-3}T^2 \quad (26)$$

$$L_2 = 40.49 + 1.357T + 3.688 \cdot 10^{-3}T^2 \quad (27)$$

$$u_1 = [L_1 - (AL_1 + B)\sqrt{c/1000}]/10000F \quad (28)$$

$$u_2 = [L_2 - (AL_2 + B)\sqrt{c/1000}]/10000F \quad (29)$$

where c is the concentration in mol m^3, T is the temperature in °C and u_1 and u_2 are the mobilities in $m^2\ V^{-1}\ s^{-1}$.

Analogously, for the temperature dependence of the diffusion coefficients we obtained

$$D_1 = 4.195 \cdot 10^{-9}(T + 273)\exp\left(-\frac{2040}{T + 273}\right) \quad (30)$$

$$D_2 = 6.396 \cdot 10^{-9}(T + 273)\exp\left(-\frac{2040}{T + 273}\right) \quad (31)$$

where D_1 and D_2 are the diffusion coefficients in $m^2\ s^{-1}$.

For very dilute solutions, the heat is transported in a capillary column mainly by the solvent, and therefore values valid for water were taken as constants, namely $\rho_m = 1000$ kg m^{-3} and $c_h = 4187$ J K^{-1} kg^{-1}. The thermal conductivity of water varies slightly with temperature from 0.56 W K^{-1} m^{-1} at 0°C to 0.68 W K^{-1} m^{-1} at 100°C. In this work, an average value of $K = 0.6$ W K^{-1} m^{-1} was considered. The thermal conductivity of the PTFE wall of the capillary tube was assumed to be $K_w = 0.27$ W K^{-1} m^{-1}.

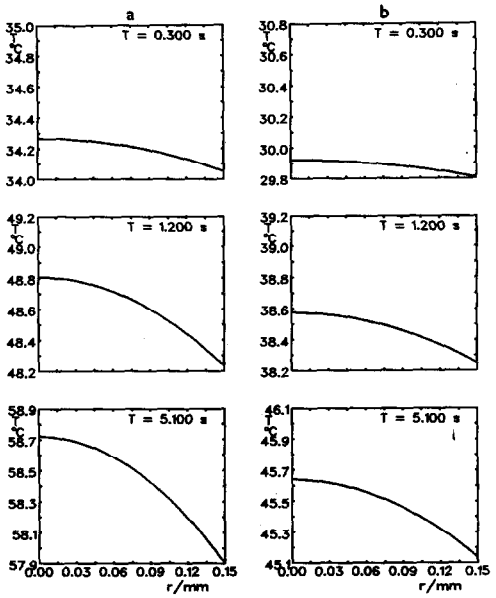

Fig. 1. Radial temperature profile in the capillary tube. Current density, −1373 A m^{-2}; temperature of surroundings, 25°C; PTFE capillary of I.D. 0.3 mm, O.D. 0.5 mm; thermal conductivity of the PTFE wall, 0.27 W K^{-1} m^{-1}; surface heat transfer coefficient, 130 W m^{-2} K^{-1}. T = temperature; r = radial coordinate of the capillary tube; t = time. (a) 1 m*M* NaCl; (b) 2 m*M* NaCl.

Computer solution of the general model

A general numerical solution of the set of eqns. 5 and 7 will be published elsewhere. For the purpose of this paper, the calculation will be limited to a uni–univalent electrolyte and cases of constant initial axial and radial distribution of concentration in the capillary, *i.e.*,

$$c(x, r, 0) = C\,, \quad T(x, r, 0) = T_S\,, \quad x \in \langle 0, L \rangle\,,$$
$$r \in \langle 0, R \rangle \tag{32}$$

where C is the initial concentration of the electrolyte.

Fig. 1 shows the radial temperature profile at various times attained by solution of eqns. 5 and 7 for two different concentrations of sodium chloride, namely 1 and 2 mol m^{-3}, and assuming the initial conditions in eqn. 32. At time $t = 5.1$ s, the radial temperature profile is almost in a steady state. It is seen that the temperature difference between the centre and the wall of the capillary is less than 1°C, whereas that between the two solutions is about 13°C.

Computer solution of the simplified model

The simplified model in eqns. 20 and 21 has the advantage of a fairly rapid numerical solution and less computer memory requirement, but nevertheless still seems to be able to describe main "axial features" of the general model.

The solution reveals the existence of two interesting effects: oscillation of the concentration profile on concentration boundaries and changes in concentration of the electrolytes (either an increase or a decrease) appearing at sites of jumps of the overall heat transfer coefficient h_0.

Oscillation of the concentration profile. The numerical solution of eqns. 20 and 21, with initial and boundary conditions in eqns. 22 and 23 and assuming a constant heat transfer coefficient along the capillary tube, is demonstrated in Fig. 2. In this and analogous figures, the initial distribution of concentration shown in (a) is the initial condition. The triad (a), (b) and (c) shows the time development of a moving concentration boundary between $c' = 2$ mol m^{-3} and $c'' = 4$ mol m^{-3} NaCl in an air-cooled PTFE capillary of I.D. 0.3 mm and O.D. 0.5 mm. The linear

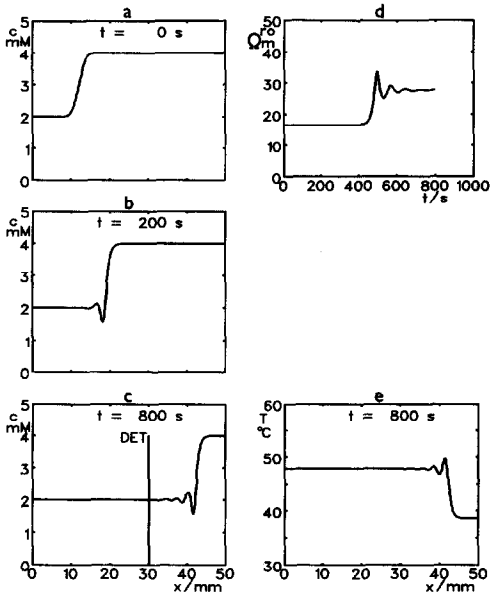

Fig. 2. Simulation of electromigration of the boundary between 2 and 4 mM NaCl. Current density, −1500 A m^{-2}; temperature of surroundings, 25°C; PTFE capillary of I.D. 0.3 mm, O.D. 0.5 mm; thermal conductivity of the PTFE wall, 0.27 W K^{-1} m^{-1}; surface heat transfer coefficient, 130 W m^{-2} K^{-1}. c = Concentration; r_0 = specific resistance; T = temperature; x = axial coordinate of the capillary tube; t = time; DET = position of the detector. (a), (b), (c) Distributions of concentration in the capillary tube; (d) time record of the specific resistance measured by the detector at a position 30 mm along the capillary tube; (e) distribution of temperature in the capillary tube.

velocity, v, of the boundary according to Stockmayer [11] is

$$v = \frac{j(N' - N'')}{F(c' - c'')} \tag{33}$$

where N' and N'' are the transference numbers of sodium in the two solutions with concentrations c' and c'' and the transference number N is expressed as $N = u_1/(u_1 + u_2)$. In Fig. 2, the transference numbers resulting from eqns. 28 and 29 are $N' = 0.40042$ and $N'' = 0.39544$ and, hence, the velocity of the concentration boundary calculated by eqn. 33 is $v = 38.7 \cdot 10^{-6}$ m/s. This value corresponds well with the velocity of the boundary deduced from Fig. 2. With the direction of the electric current used, $j = -1500$ A m^2, the temperature gradient facilitates main-

taining the boundary width in a steady state, *i.e.*, it has a sharpening effect. Additionally, moving dumped oscillations of the profile appear on the trailing edge of the boundary. Fig. 2 also shows the axial temperature profile (e) corresponding to a given time and the time record (d) of the signal of a conductivity detector placed at a position 30 mm along the capillary tube.

If the current is in the opposite direction towards the concentration boundary (Fig. 3), only small oscillations are observed and the moving boundary is spread more rapidly than in the case of free diffusion.

Both sharpening and spreading effects have been described previously [10,11] for electromigration not influenced by Joule heat evaluation. Nevertheless, they can be much more pronounced if the heat evaluation plays a significant role.

Eqns. 20 and 21 are non-linear, hence their solution depends non-linearly on the initial and boundary conditions. On changing the concentration of the solution and the electric current density (Figs. 4–6), further patterns of the concentration profile moving in the capillary can be seen. Fig. 4 reveals a slight irregularity in the oscillations, Fig. 5 shows a series of sharp per-

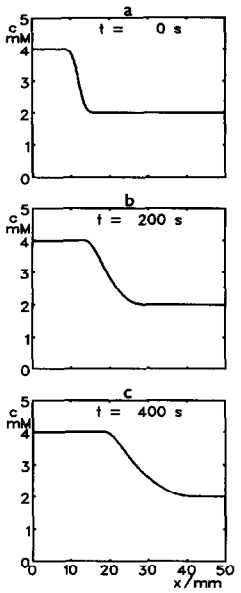

Fig. 3. Simulation of electromigration of the boundary between 4 and 2 m*M* NaCl. Current density, -1500 A m^{-2}; temperature of surroundings, 25°C; PTFE capillary of I.D. 0.3 mm, O.D. 0.5 mm; thermal conductivity of the PTFE wall, 0.27 W K^{-1} m^{-1}; surface heat transfer coefficient, 130 W m^{-2} K^{-1}. c = Concentration; x = axial coordinate of the capillary tube; t = time. (a), (b), (c) Distributions of concentration in the capillary tube.

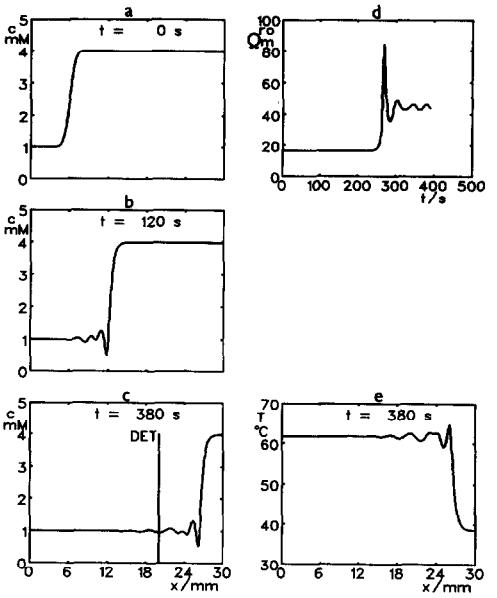

Fig. 4. Simulation of electromigration of the boundary between 1 and 4 m*M* NaCl. Details as in Fig. 2.

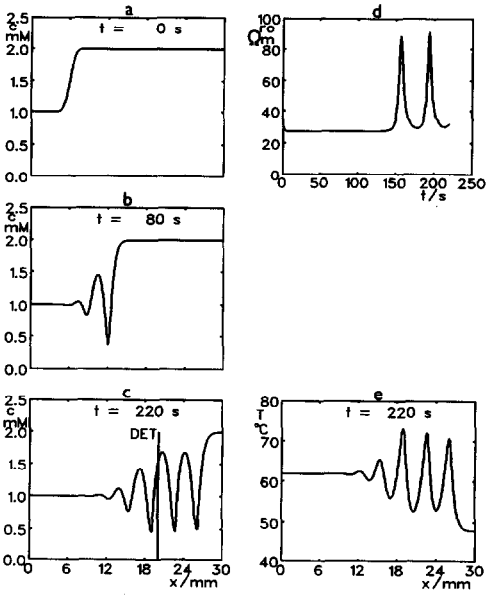

Fig. 5. Simulation of electromigration of the boundary between 1 and 2 m*M* NaCl. Details as in Fig. 2.

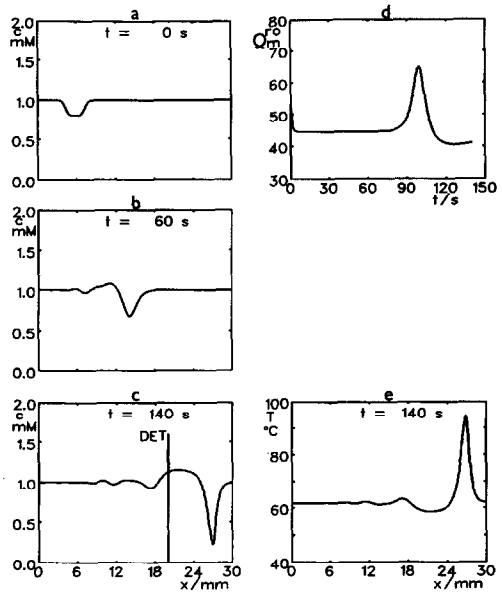

Fig. 6. Simulation of electromigration of a small concentration disturbance in 1 m*M* NaCl. Details as in Fig. 2.

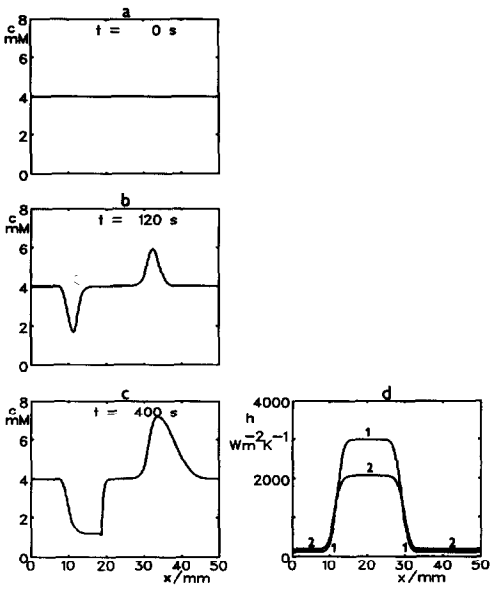

Fig. 7. Simulation of concentration development at the sites of two jumps in the radial heat transfer. Current density, -1500 A m^{-2}; temperature of surroundings, 25°C; PTFE capillary of I.D. 0.3 mm, O.D. 0.5 mm; thermal conductivity of the PTFE wall, 0.27 W K^{-1} m^{-1}. c = Concentration; x = axial coordinate of the capillary tube; t = time; h = heat transfer coefficient. (a), (b), (c) Distributions of concentration in the capillary tube; (d) axial profiles of the heat transfer coefficients. 1 = Surface heat transfer coefficient; 2 = overall heat transfer coefficient.

iodic dips that may move stably in a capillary tube and Fig. 6 demonstrates that if the current density is sufficiently high for a given concentration, even a small disturbance in the concentration profile is quickly amplified.

Changes in concentration at jumps of the overall heat transfer coefficient. The overall heat transfer coefficient h_0 may not be constant along the capillary, *i.e.*, it may be a function of the x-coordinate. Jumps of the heat flux through the capillary wall may often occur in practice at junctions of tubing.

Fig. 7 shows a simulation of the concentration development at the sites of two jumps of h_S (from 130 to 3200 W m^{-2} K^{-1} and *vice versa*). This corresponds to an illustrative situation where an air-cooled capillary tube is partly immersed in cooling water. The axial profiles of h_S and h_0 are shown in Fig. 7d for the PTFE capillary of I.D. 0.3 mm and O.D. 0.5 mm. A constant initial distribution of concentration in the capillary is assumed. The concentration decreases at the site of the left jump, whereas it increases at the site of the right jump. Both sites therefore generate concentration boundaries that move in the capillary as in previous cases and that can cause oscillations. This is shown in Fig. 8, where the jump in radial heat flux may be a source of moving sharp oscillations.

If the electric current exceeds a certain value, a decrease in concentration occurs and the temperature tends to exceed the boiling point of the solution. In reality, boiling of the solution at such a site leads immediately to the breaking of the electric current. It seems that this mechanism of breaking of the current will be more probable than the axial mechanism of autothermal runaway described by Gobie and Ivory [8]. This is supported by the practical observation that an occasional "trip" during electrophoretic experiments frequently occurs at one junction between a capillary tube and an electrode vessel where the radial heat flux exhibits a large jump. If the electric current is in the opposite direction, the trip takes place at the junction of the other electrode vessel (or on another jump of heat resistance).

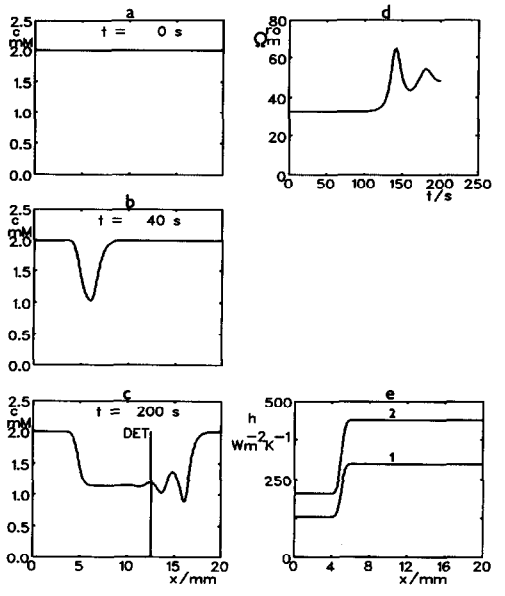

Fig. 8. Generation of oscillations at a jump in the radial heat transfer. Current density, -1500 A m^{-2}; temperature of surroundings, 25°C; PTFE capillary of I.D. 0.3 mm, O.D. 0.5 mm; thermal conductivity of the PTFE wall, 0.27 W K^{-1} m^{-1}. c = Concentration; x = axial coordinate of the capillary tube; t = time; h = heat transfer coefficient. (a), (b), (c) Distributions of concentration in the capillary tube; (d) time record of the specific resistance measured by the detector at a position 12.5 mm along the capillary tube; (e) axial profiles of the heat transfer coefficients. 1 = Surface heat transfer coefficient; 2 = overall heat transfer coefficient.

Linear model

For a better understanding of the origin of the oscillations, eqns. 20 and 21 can be converted into a linear form, which is of course only approximate but able to reveal substantial terms responsible for oscillations.

Assuming a constant current density j, diffusion coefficient D and thermal conductivity K, eqns. 20 and 21 can be rewritten accordingly:

$$\frac{\partial c}{\partial t} = D \cdot \frac{\partial^2 c}{\partial x^2} - \frac{j}{F} \cdot \frac{\partial}{\partial x}\left(\frac{u_1}{u_1 + u_2}\right) \tag{34}$$

$$\rho_m c_h \cdot \frac{\partial T}{\partial t} = K \cdot \frac{\partial^2 T}{\partial x^2} + \frac{j^2}{Fc(u_1 + u_2)} - h_0 \cdot \frac{2}{R}(T - T_S) \tag{35}$$

It can be shown that for every reasonable value of c there is a unique T satisfying

$$\frac{j^2}{F(u_1 + u_2)c} - h_0 \cdot \frac{2}{R}(T - T_S) = 0 \tag{36}$$

where u_1 and u_2 are given by eqns. 28 and 29. The value of T obtained by solving eqn. 36 is a function of c, say $T = T(c)$, and represents the value to which the temperature of a system with an axially homogenous concentration c stabilizes when t tends to infinity. If we took just the function $T(c)$ and inserted it in eqn. 34, we would reduce the pair of eqns. 34 and 35 to an equation for c but the phenomena found when studying the full system would not appear. This is a consequence of the maximum principle for parabolic equations. It proves the importance of eqn. 35 in the process. It seems that in the behaviour of the full system of eqns. 34 and 35 it is very important that, in some way, the temperature lags behind the concentration.

As the initial concentration profile we take $c(x,0) = \gamma(1000x - 8)$, where

$$\begin{aligned} \gamma(\xi) &= 1 && \text{for } \xi < -1 \\ &= \frac{1}{2}\left[\frac{\sin(\pi\xi)}{\pi} + \xi + 3\right] && \text{for } -1 \leq \xi \leq 1 \\ &= 2 && \text{for } \xi > 1 \end{aligned} \tag{37}$$

If $c = 1.5$, the "average" value of the initial concentration and $j = -1373$, $h_0 = 200$, $T_S = 25$, $R = 0.15 \cdot 10^{-3}$, we find from eqns. 36 and 24–29 that $T = T_S + 25$. These values will be used when arranging terms in eqns. 34 and 35. For $N(c, T) = u_1/(u_1 + u_2)$, the transference number, this means that

$$-\frac{j}{F} \cdot \frac{\partial N}{\partial x} = -\frac{j}{F}\left(\frac{\partial N}{\partial c} \cdot \frac{\partial c}{\partial x} + \frac{\partial N}{\partial T} \cdot \frac{\partial T}{\partial x}\right) = -V \cdot \frac{\partial c}{\partial x} + M \cdot \frac{\partial T}{\partial x} \tag{38}$$

where the values of V and M can be found from eqns. 24–29 and are $V = 1.910 \cdot 10^{-5}$ and $M = 4.476 \cdot 10^{-6}$.

Linearizing $1/c$ around $c = 3/2$, we obtain $1/c \approx (4/9)(3 - c)$ and the system of eqns. 34 and 35 changes to

$$\frac{\partial c}{\partial t} = D \cdot \frac{\partial^2 c}{\partial x^2} - V \cdot \frac{\partial c}{\partial x} + M \cdot \frac{\partial T}{\partial x} \tag{39}$$

$$\frac{\partial T}{\partial t} = \alpha \cdot \frac{\partial^2 T}{\partial x^2} + \beta\left[\frac{50}{3}(3 - c) - (T - T_S)\right] \tag{40}$$

where $D = 1.50 \cdot 10^{-9}$, $\alpha = 1.4 \cdot 10^{-7}$ and $\beta = 0.6274$. Finally, as the initial conditions are taken

$$c(x, 0) = \gamma(1000x - 8) \quad (41)$$

$$T(x, 0) = T_S + 50 - \frac{50}{3} c(x, 0) \quad (42)$$

Eqn. 42 gives the initial temperature distribution to which the temperature governed by eqn. 40 would stabilize if the concentration in the capillary were $c(x, 0)$.

The system of eqns. 39–42 was studied on the real line, *i.e.*, for $x \in (-\infty, \infty)$ by applying Fourier transformation. The solution of the transformed equation can be inverted numerically for any value of time and thus the evolution of the concentration profile governed by eqns. 39–42 can be obtained.

Fig. 9 presents the results of three different computations for comparison. Curve 1 is the result of the Fourier transform solution of the linear eqns. 39–42, curve 2 is the result of the numerical solution of the linear eqns. 39–42 and curve 3 is the result of the numerical solution of the original non-linear eqns. 20 and 21 using the initial conditions 41 and 42 and with $j = -1373$, $h_0 = 200$, $T_S = 25$ and $R = 0.15 \cdot 10^{-3}$. There is perfect agreement between both solutions of the linear problem and very good qualitative agreement with the non-linear solution.

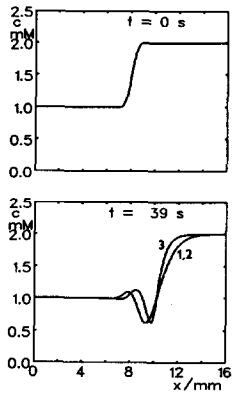

Fig. 9. Comparison of various solutions of differential equations. Current density, -1373 A m^{-2}; temperature of surroundings, 25°C; overall heat transfer coefficient, 200 W m^{-2} K^{-1}. x = Axial coordinate of the capillary tube; t = time. (a) Initial condition eqn. 41; (b) results. 1 = Result of the Fourier transform solution of the linear eqns. 39–42; 2 = result of the numerical solution of the linear eqns. 39–42; 3 = result of the numerical solution of the non-linear eqns. 21 and 22 using the initial conditions 41 and 42.

On the basis of the results, it can be stated that the phenomena found when studying the full non-linear system are also found in the linearized problem.

It can be concluded, that, according to Stockmayer [11], the concentration boundary moves if the transference number depends on concentration. Additionally, the moving oscillations of the concentration profile can appear if the transference number is dependent on temperature, even if this dependence is linear.

Similarly, a non-linear nature of the system is not essential for the increase and decrease in concentration on jumps in the overall heat transfer coefficient. They can appear whenever a transference number is dependent on temperature, even if this dependence is linear.

Experimental verification

The theoretically predicted phenomena were supported experimentally.

Oscillation phenomena frequently occur in practice and are often misinterpreted as artifacts of contact conductivity detectors. Fig. 10 shows the records of a high-frequency contactless conductivity detector, revealing examples of such oscillations. The oscillations appear several minutes after switching an electric current. The high-frequency detector has the advantage of contactless conductivity measurement, hence electrode reactions that would disturb measurements are prevented. On the other hand, it should be emphasized that most construction designs of conductivity detectors alter the radial flux of the capillary wall, which therefore causes the above-mentioned jumps in the radial heat flux and, consequently, sites where a decrease or increase in concentration may occur. The measuring cell of the high-frequency contactless conductivity detector used (similar to that described previously [22]) is formed by a brass cylinder with measuring electrodes. A PTFE capillary tube is fed through the axial hole in the cylinder. It implies the origination of two jumps in the heat flux at both ends of the cylinder. In addition, other sites of such jumps are at every junction of tubing. Apparently, these jumps are sources of the observed oscillations.

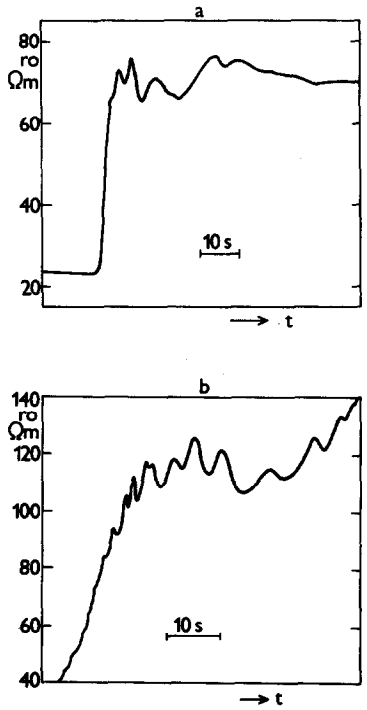

Fig. 10. Experimental record of the conductivity detector. Electrolyte solution in the whole system (*i.e.*, in anodic and cathodic vessels and in the capillary tube), 4 m*M* NaCl. PTFE capillary of I.D. 0.4 mm, O.D. 0.6 mm. r_0 = Specific resistance; t = time. (a) Current 180 μA, cathode at the sample side, anode at the detector side; (b) current 180 μA, anode at the sample side, cathode at the detector side.

The decrease or increase in concentration at jumps of the surface heat transfer coefficient can be verified in an experiment checking the simulation described in Fig. 7. Such an experiment can be realized on a common isotachophoretic instrument using a PTFE capillary of I.D. 0.3 mm and O.D. 0.5 mm. A cathodic and anodic vessel and the capillary are filled with a 4 mol m^{-3} solution of sodium chloride and the capillary is partly immersed in a cooling water-bath. The schematic arrangement of this experiment is shown in Fig. 11. After about 3 min using a constant electric current of 200 μA, the concentration of the sodium chloride will be decreased at the site marked 5 in Fig. 11. At this site, the production of heat is higher but, owing to intensive water cooling, the temperature at this site does not exceed the boiling point of the solution. However, after removing the capillary

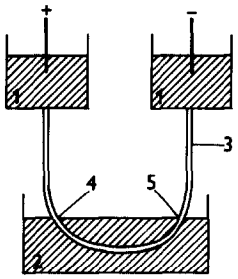

Fig. 11. Arrangement of the experimental check of the increase and decrease in concentration at jumps in the radial heat transfer. 1 = Anodic and cathodic compartments filled with electrolyte; 2 = cooling water; 3 = capillary tube; 4,5 = sites of concentration changes.

from the water-bath and maintaining the same electric current, a break in the current takes place after a few seconds.

The decrease or increase in concentration at jumps of the surface heat transfer coefficient can also be visualized if an ionic organic dye, *e.g.*, bromophenol blue, is used as an electrolyte in the electrophoretic experiment with the same arrangement as shown in Fig. 11 but with a thicker capillary tube, *e.g.*, of I.D. 0.8 mm, for better visibility. Bleaching is observed at the site marked 4 in Fig. 11 and, *vice versa*, there is a deepening of the colour at site 5. Bromophenol blue is a weak acid with $pK_A \approx 3.8$. Detailed temperature dependences of the mobility and diffusion coefficient of its anionic form or the temperature dependence of the pK_A value are not known. Nevertheless, it can be expected that the properties of the cationic and anionic constituents of the dye will differ and the dye will have an analogous migration behaviour to a solution of NaCl.

APPENDIX

Let us check whether the above-mentioned neglect of the Soret effect [13] (and the Dufour effect) [13]) plays a significant role in the described model of electromigration. Assuming a very dilute solution of a strong binary electrolyte, the thermodynamic force X_i ($i = 1, 2$) raising the mass flux of the ith ion in solution in the electric field can be written [12] according to the Onsager theory as

$$X_i = -\frac{RT}{c_i}\cdot\frac{\partial c_i}{\partial x} - \mathrm{sgn}(z_i)F\cdot\frac{\partial \phi}{\partial x} \quad (43)$$

The thermodynamic force X_3 raising the heat flux is

$$X_3 = -\frac{1}{T}\cdot\frac{\partial T}{\partial x} \quad (44)$$

Hence the fluxes J_1 and J_2 of ions 1 and 2 and flux J_3 of the heat are

$$J_1 = L_{11}X_1 + L_{12}X_2 + L_{13}X_3 \quad (45)$$

$$J_2 = L_{21}X_1 + L_{22}X_2 + L_{23}X_3 \quad (46)$$

$$J_3 = L_{31}X_1 + L_{32}X_2 + L_{33}X_3 \quad (47)$$

where L_{ij} (i, $j = 1, 2, 3$) are phenomenological Onsager coefficients. The Onsager reciprocity theorem declares $L_{ij} = L_{ji}$. In our case with very dilute solution, the interaction between ions can be neglected to a good approximation, *i.e.*, $L_{12} = L_{21} = 0$. The remaining non-diagonal coefficients L_{13}, L_{23}, L_{31} and L_{32} are responsible for the Soret and Dufour effects.

Eqns. 45 and 46 can be rewritten using eqn. 2 and the electroneutrality condition declaring $c_1 = c_2 = c$. Using further relationships between phenomenological and diffusion coefficients [13,16], the individual mass fluxes are (for the case of a uni–univalent electrolyte)

$$J_i = -D\left(\frac{\partial c}{\partial x} + sc\cdot\frac{\partial T}{\partial x}\right) + \mathrm{sgn}(z_i)\cdot\frac{u_i}{u_1+u_2}\cdot\frac{j}{F} \quad (48)$$

where $i = 1, 2$ and s is the Soret coefficient. The Soret coefficient of an electrolyte solution is strongly dependent on temperature. Its value is approximately several 10^{-3} K^{-1} for our solutions of NaCl in the temperature range 20–50°C. Knowing the value of the Soret coefficient, it is possible to calculate the term $sc\,\partial T/\partial x$ in the previously calculated results and compare it with the $\partial c/\partial x$ term. This can be done, *e.g.*, for the results shown in Fig. 5. In Fig. 12 there are plotted both terms assuming a value of the Soret coefficient of 0.005 K^{-1} and it is obvious that the amplitude of the $\partial c/\partial x$ term is much greater (about ten times) than the amplitude of the $sc\,\partial T/\partial x$ term.

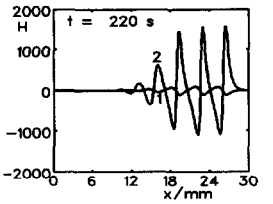

Fig. 12. Plot of $sc\,\partial T/\partial x$ and $\partial c/\partial x$ terms for the situation simulated in Fig. 5. x = Axial coordinate of the capillary tube; t = time. 1 = $sc\,\partial T/\partial x$ term; 2 = $\partial c/\partial x$ term; H = value of the terms in mol m^{-4}.

From this, it can be assumed that neglect of the Soret effect did not cause significant errors in the previous calculations. Analogously, the same would be valid for the flux of the heat and the Dufour effect.

ACKNOWLEDGEMENT

Dr. Milan Štědrý of the Faculty of Science, Charles University, Prague, is thanked for his kind assistance with the mathematical work.

REFERENCES

1 S. Hjertén, *Chromatogr. Rev.*, 9 (1967) 122.
2 M. Coxon and M.J. Binder, *J. Chromatogr.*, 101 (1974) 1.
3 J.F. Brown and J.O.N. Hinckley, *J. Chromatogr.*, 109 (1975) 218.
4 J.H. Knox and I.H. Grant, *Chromatographia*, 24 (1987) 135.
5 F. Foret, M. Deml and P. Boček, *J. Chromatogr.*, 452 (1988) 601.
6 E. Grushka, R.M. McCormick and J.J. Kirkland, *Anal. Chem.*, 61 (1989) 241.
7 A.E. Jones and E. Grushka, *J. Chromatogr.*, 466 (1989) 219.
8 W.A. Gobie and C.F. Ivory, *J. Chromatogr.*, 516 (1990) 191.
9 J.M. Davis, *J. Chromatogr.*, 517 (1990) 521.
10 L.G. Longsworth, *J. Am. Chem. Soc.*, 65 (1943) 1755.
11 W.H. Stockmayer, *Trans. N.Y. Acad. Sci.*, 13 (1951) 226.
12 K.G. Denbigh, *The Thermodynamics of the Steady State*, Methuen, London, New York, 1951.
13 R. Haase, *Thermodynamik der Irreversiblen Prozesse*, Dr. Dietrich Steinkopf, Darmstadt, 1963.
14 I. Prigogine, *Introduction to Thermodynamics of Irreversible Processes*, Interscience, New York, 1967.
15 H.S. Carslaw and J.C. Jaeger, *Conduction of Heat in Solids*, Clarendon Press, Oxford, 2nd ed., 1986.

16 T. Erdey-Grúz, *Transport Phenomena in Aqueous Solutions*, Akadémiai Kiadó, Budapest, 1974.
17 L. Onsager and R.M. Fuoss, *J. Phys. Chem.*, 36 (1932) 2689.
18 P.W. Atkins, *Physical Chemistry*, Oxford University Press, Oxford, 4th ed., 1990.
19 R.B. Bird, W.E. Stewart and E.N. Lightfoot, *Transport Phenomena*, Wiley, New York, 1960.
20 E.V. Dose and G.A. Guiochon, *Anal. Chem.*, 63 (1991) 1063.
21 A. Ralston, *A First Course in Numerical Methods*, McGraw-Hill, New York, 1965.
22 B. Gaš, M. Demjaněnko and J. Vacík, *J. Chromatogr.*, 192 (1980) 253.
23 B.E. Conway, *Electrochemical Data*, Elsevier, Amsterdam, 1952.